VOL. 15, NO. 15, AUGUST 2020 ISSN 1819-6608
ARPN Journal of Engineering and Applied Sciences

www.arpnjournals.com

MATHEMATICAL SIMULATION OF INTERNAL PROCESSES OF SOIL CUTTING WITH ACCOUNTING FOR SIDING SURFACE

Kuanysh Turusbekov, Ermek Abilmaginov, Yerzhan Shayakhmetov, Dalel Zhailaubaev and Rysbala Ibragimova
Shakarim State University of Semey, St. Glinka 20A, Semey, East Kazakhstan region, Republic of Kazakhstan
E-Mail: kuanturus@mail.ru

ABSTRACT

This article describes the energy intensity of soil excavation and variations of cutting effort constituents acting on manipulator which are required for effective interaction with soil. Internal processes of soil cutting are analyzed upon processing of various soils. The schemes of manipulator interaction with soil are considered since they are important both for analysis of operation of existing earthmoving machinery and for development of new units. Studying volumetric soil cutting by earthmoving manipulator is a contact, elastic and plastic, nonlinear problem with accounting for temperature mode of deformation. The required horizontal and vertical constituents of cutting forces, temperature field, and soil flow rate upon one pass of manipulator have been predicted with accounting for sliding surface. The methods and equations of limit equilibrium theory have been applied resulting in derivation of equations of soil resistance against cutting. The results are confirmed by substantiated use of fundamental dependences, assumptions and limitations, correct formulation of mathematical simulation, application of modern mathematical methods and hardware. The predicted and experimental data on resistance against cutting of various soils are presented with regard to practical range of applied cutting angles for knife manipulators of earthmoving machinery.

Keywords: blade, bulldozer, cutting soil, earthmoving machines, soil.

INTRODUCTION

Engineering advances in the field of earthmoving and excavating machinery for soils of various mechanical properties are aimed at improvement of efficiency of processing manipulators. The efficiency of road construction machinery regarding earth extraction depends on complete implementation of their specifications under operation properties defined by a set of indices. Efficiency of the machinery can be improved by their sustainable use regarding their capacity and time. The first trend is based on determination, analysis, and optimization of operation properties of certain earthmoving machines, including traction properties and application of manipulators (Figure-1). The second trend is based on development and improvement of effective parameters of manipulators, operation modes of earthmoving machines, as well as theoretical foundations of interaction with working media.

Figure-1. Manipulators of road construction machinery for earth excavation.

Experimental and analytical results of mathematical models of operation processes of road construction machinery are of great importance for designing and development of new challenging machinery, they are reliable basis for implementation of efficient technologies.

Taking into consideration the present importance of improvement of excavation activities of road construction, the authors studied a method of soil mechanical destruction accounting for sliding surface. Investigation into soil cutting is related with wide scope of theoretical and experimental studies resulting in necessity to improve predictions of soil resistance, energy intensity during production of manipulators as well as determination of main variables. These methods are described insufficiently in available publications, they require for thorough studies.

This predetermined necessity to consider theoretically interaction of a manipulator with soil aiming at subsequent correction of predictions of cutting forces and soil resistance during processing as well as energy intensity of cutting and selection of working variables for designing of manipulators with accounting for peculiar features of cutting.

The aim of this work is improvement of predictions of soil resistance against cutting by earthmoving manipulator by adjustment of shape of sliding surface; decrease in energy intensity of soil excavation; expansion of operation capabilities; expansion of application area; equipment controllability; increase in reliability; increase in productivity; simplification of design; expansion of engineering capabilities. The main aim of analysis of soil cutting is searching for methods of the low energy and the most productive separation of soil from solids.

The manipulators of earthmoving machines during interaction with soil are exerted to random loads varying in time. Depending on manipulator type, soil and other conditions, the random loads are different. Therefore, it is important to classify both these processes and manipulators of earthmoving machines depending on type of random process.

General classification of random processes of loads acting on manipulators of earthmoving machines can be based on the following main properties: stationary/nonstationary; ergodic/non-ergodic; type of distribution of instant values of the considered parameter; differentiable/nondifferentiable.

Such classification allows to apply main statistical properties and similar random load properties for analysis and evaluation not only of each manipulator of earthmoving machine but also for groups of manipulators under similar loads.

THEORETICAL SUBSTANTIATION

Soil cutting is comprised of soil separation from solids by cutting manipulators not intended for soil transportation. Cutting is characterized by absence of drawing prism and possibility to track daily soil surface up to chip removal from cutting manipulator surface.

In construction industry the soils are mainly foundation for various structures, which should perform their functions upon any combinations of natural impacts (moisture, solar radiation, wind). Therefore, the project designing is based on analysis of physicomechanical properties of soils of assumed position of construction site.

Soil is comprised of any rock, ground, solid wastes of industrial and human business activities used as foundation upon erection of buildings and engineering facilities.

Properties of soils are determined by their structure, porosity, particle size distribution, and moisture content. The particle size distribution is determined by percentage of particles and stone inclusions of the following sizes (Table-1).

Table-1. Ratio of particles and stone inclusions.

Description	Particle sizes
Boulders	more than 20 cm
Cobblestone	4...20 cm
Gravel	2...40 mm
Sand	0.05...2 mm
Dust	0.005...0.05 mm
Clay	less than 0.005 mm

The mechanical properties of soils are significantly affected by moisture content determined by the weight moisture ω: the ratio of water weight G_W in soil sample to the sample weight after drying G_D:

$$\omega = \frac{G_W}{G_D} \cdot 100\% = \frac{G - G_D}{G_D} \cdot 100\%, \quad (1)$$

where G is the weight of wet sample.

The following moisture content can be distinguished (Table-2):

hygroscopic (a soil particle is coated with water film with the thickness of one molecule);

molecular (a soil particle can hold water film of maximum thickness due to molecular forces;

capillary (water fills the thinnest capillaries between soil particles);

gravitational (moisture content above capillary one).

Table-2. Moisture content of various soils, ω%.

Soil	Hygroscopic	Molecular	Capillary
Sand	1.5...3	5...6	7...8
Sand clay	3...6	8...12	12...15
Clay loam	6...8	12...15	15...20
Clay	8...13	1...20	20...28

In addition to strength, the weight moisture effects adhesion P_{ad} (n/cm^2) of soils (capability of soils to adhere with manipulator coating). It is established that the highest adhesion is that of clays at moisture content lower than the yield strength ω_T. Adhesion as a function of moisture content is illustrated in Figure-2.

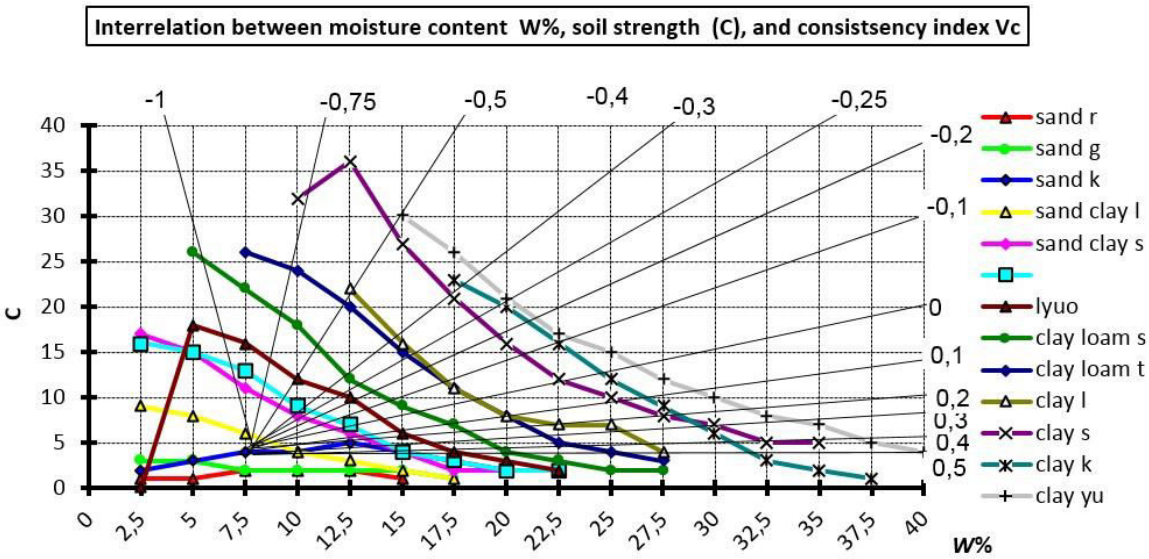

Figure-2. Adhesion as a function of moisture content.

The author [1] also provides the spread velocity value of the plastic deformations (Figure 3) as a variable characterizing the physical and mechanical properties of the soil. It is associated with the cutting speed by the following relationship:

$$\vartheta_d = \vartheta \frac{\sin\delta}{sin(\delta + \theta)} \quad (2)$$

It is assumed that during the digging the angle between the sliding surfaces and the surface of the soil mass slightly deviates from the cleavage at the angle of θ. At the same angle forming elements of the conical surfaces are tilt to the soil mass plane.

The front part of the moldboard blade compresses the soil and in the point of contact plastic deformations develop. The more is the contact of the surface of the moldboard blade with the soil, the more shear stress is. If the values exceed the values corresponding to the limit state, there is a shift of the sliding surface. The plastic formations reach the highest values on the destruction surface *ST*.

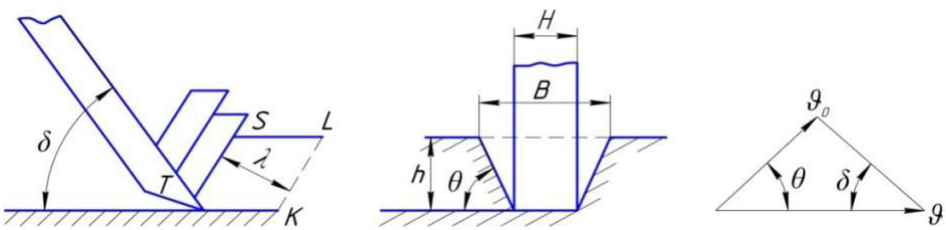

Figure-3. Shift of sliding surface upon increased contact of knife with soil.

Interaction of manipulators with soil depends on manipulator purposes, its design and geometrical parameters (shape and sizes, shape of cutting elements and sharpening angle), kinematic peculiarities of digging machine, parameters of removed chip (width, thickness and their ratios, transversal surface area) and flowchart of interaction of manipulators with soil (number of opened surfaces of excavated bulk), physicomechanical properties of soil, and others. Generally, interaction of manipulators with soil results in deformations of compression, shift, and tension of soil accompanied by its breakage as well as friction of soil upon its movement on manipulator surface, friction of manipulator on soil, and friction of soil on soil.

Interactions of digging manipulators with soil are extremely complicated: they result in soil deformations of all types, attrition on manipulator surface and on soil. Upon insertion of manipulators (continuously for some manipulators), friction also occurs between back and lower edges of cutting element and soil. The main processes occurring upon interaction of various manipulators with soil are described by Berestov E.I. [2]. The important constituent of digging is resistance against cutting, which in its turn is characterized by multiparameter function depending on design parameters of manipulators, their operation modes and physicomechanical properties of soils.

Upon movement of cutting tool, the soil bulk is deformed, and upon reaching ultimate strength, there occurs breakage of soil structural bonds or its plastical deformation resulting in cleavage of certain amount of soil. With other conditions being equal, the soil resistance against cutting is determined mainly by sliding surface

ARPN Journal of Engineering and Applied Sciences

during chip separation from soil bulk. "Sliding surfaces, along which element of material is separated from the bulk in each case, are characterized by the shape corresponding to motion direction with the minimum resistance" [3-6].

The type of sliding surface depends on properties of soils, it is difficult to determine it because of their variety. Therefore, while discussing the methods of determination of soil resistance against cutting, researchers have selected the following: specific soil resistance against cutting which depends also on designs of manipulators, number of impacts of density meter. These variables are not expressed analytically and should be established experimentally for sufficiently wide range of soils in each specific case.

Numerous experimental studies of sliding surfaces were performed by Prof. A.N. Zelenin. Based on the experimental results, A.N. Zelenin has discovered that the sliding surfaces independently on cutting angle are comprised of a series of curves which are perpendicular to cutting edge in its vicinity, and in the soil bulk they are deviated more and more upwards to open surface.

Based on the works by A. N. Zelenin, the empirical equation was proposed for evaluation of tangential constituent of soil resistance against cutting:

$$P = c \cdot h^{1,35} \cdot (1 + 2,6 \cdot b) \cdot (1 + 0,0075 \cdot \alpha) \cdot z \cdot \mu \quad (3)$$

where: c was the soil constant; α was the cutting angle, degrees; z was the coefficient accounting for the influence of teeth; μ was the coefficient characterizing the influence of number of blocked sides of cut. Variables h and b (cm) had the same sense.

Subsequent studies of soil cutting revealed certain limitations of Eq. (3). This circumstance is related with uncertainty of c property assumed to be generalized index of soil resistance against cutting by machines, it is manifested in the absence of proportionality between c and force of soil cutting. This can be attributed to the fact that soil resistance varies upon insertion of density meter into soil. At certain stage of insertion of density meter into soil, the work of soil elastic resistance reaches the impact energy, as a consequence, the number of impacts of dropped weight of density meter increases and approaches infinity.

At the same time, it should be mentioned that the dependence of sliding surfaces on soil properties, processing methods, and speed of application of destroying load has not been studied in details.

Along with the experimental research, some attempts have been taken to determine the digging forces analytically [1, 7-11]. The calculations results by these formulas are significantly different from the true values, but such research is suitable for the development of the correct technique for the calculation of the resistance forces to the digging in the close connection with the research of the destruction mechanism of the soils by different mechanical ways. To create a mathematical model of the process of the soil digging by the executive devices (bulldozer blade or scraper bowl) and to establish the calculation formulas for the determination of the total resistance, the researchers have taken the photographs of these processes with the use of the colored soil layers. For this purpose, the soil of the definite color was spread on the surface of the developed soil. The typical photographs of the process of the soil digging by bulldozer blade are shown in Figure-4. The process was implemented by the use of such technique.

Figure-4. The soil digging by blade, the color layers are only in the chip.

As a result, researchers have developed and offered the calculation schemes to determine the resistance to the digging by the bulldozer blade. Versions are shown in Figure 5 [7, 12, 13]. According to these calculation schemes, the chip separated from the soil mass while digging is moving up along the executive devices or inside them in the form of a monolithic body separated from the soil mass situated in the executive devices or the drawing prism. The emerging resistance forces have indirect impact on the total resistance due to the increase of the resistance forces to the separation of the soil from the mass in the case of the kentledge *p(y)*. The effect of this kentledge extends at a distance in front of the moldboard blade:

a=h(tgα+tgψ)/(tgαtgψ),

where the shift angle $\psi = \pi/4 - \varphi 2/2$ is assumed as a constant depending only on the internal friction angle of the soil.

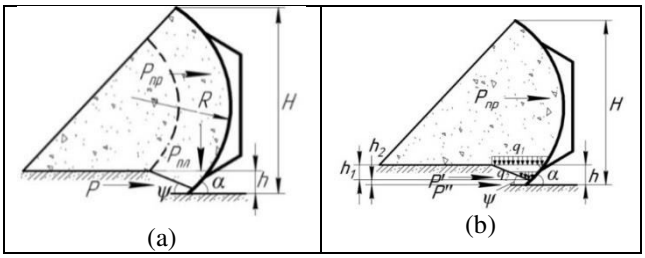

Figure-5. The calculation schemes for the determination of the resistance to the digging by bulldozer: a- the technique of V.I.Balovnev; b -the technique of G.N.Karasev.

Determining the resistance to movement of the drawing prism, the majority of the researchers consider it as a solid mass which moves along the soil surface under the executive devices. Researchers who use the limit state theory of the loosened and cohesive soils define the resistance to the movement of the prism as passive pressure on the executive devices at an angle to the horizon which is equal to the angle of the internal friction of the soil. In the determination of the resistance to the digging, the effect of the chip is not considered when it is introduced into the executive device or the drawing prism and raises a part situated there.

These experiments with color layers allow us to offer the following scheme for formation of the drawing prism (Figures 6a, b and 7) at the final stage of the process of the digging:

- in the first case (Figure 5a) the chip separated from the soil mass have such a thickness that its strength is sufficient for the introduction into the drawing prism and moving up along the surface of the blade. The chip puts the adjoining layers of the drawing prism in the motion. The part of the drawing prism AOSD rotates relative to the center the position of which is determined by the shape of the drawing prism, its height *H,* and the slope angle ρ of the drawing prism. The part of the prism ABO is stationary during the motion of the blade, but the soil layer which crumbles out of the rotating part of the prism moves along the surface BO at the angle of slope;
- in the second case (Figure 6b) the chip has such thickness that its strength is not sufficient for introduction into the drawing prism. The soil chip is separated from the soil mass by the compacted core in front of the drawing prism. In this case the drawing prism is moved by blade as a solid body which acts as an executive device. It separates the chip from soil mass and accumulates a new prism of the developed soil.

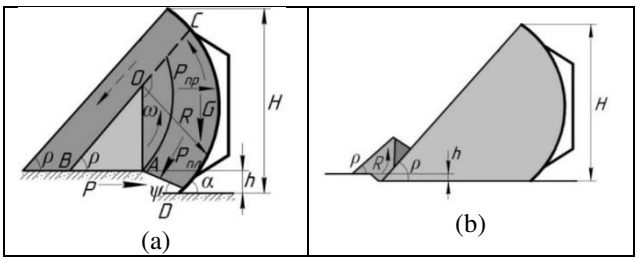

Figure-6. Schemes of the forming of the drawing prism in front of the bulldozer blade: a) the digging depth which is sufficient for the introduction of the chip into the prism; b) the small digging depth which is insufficient for the introduction of the chip into the prism;

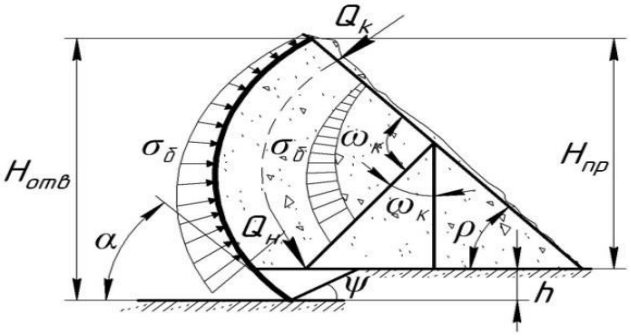

Figure-7. The calculation scheme for determination of the resistance emerging during the forming of the drawing prism.

Considering for these factors, soil cutting is presented as separation of soil chip from solids, herewith, chip is comprised of stream of continuously appearing sliding bodies moving upwards. In order to simplify predictions of forces occurring on manipulators, separation of sliding bodies from soil bulk is characterized by a plain inclined at certain angle. As a consequence, the predicted soil resistances against cutting do not agree with experimental ones, therefore, it is required to develop functional description of sliding surfaces for main soil types.

Certain aspects of soil cutting were studied by K. A. Artemiev, Yu. A. Vetrov, N. G. Dombrovskii, I. A. Nedorezov, V. K. Rudnev, L. A. Khmara, R. A. Kabashev, A. S. Kadyrov, Z. A. Moldagaliev, and others [14-18].

Therefore, up till now the aspects of influence of cutting angels, sharpening, relief angle, chip width and thickness, thickness and shape of cutting edge, manipulator design, cutting path, bucket filling, cutting speed and physicomechanical properties of soils on resistance against cutting and digging were analyzed.

Aiming at predictions of resistance against cutting, numerous researchers proposed analytical and empirical dependences, all of them were derived under certain assumptions upon selection of initial conditions and development of computational models suitable for specific application. This is attributed to differences between the predicted results based on these dependences and actual (experimental) data. It is obvious that the best agreement between soil resistances against cutting and digging based on the above dependences and experimental data should be expected in the case of equal experimental and prediction conditions.

EXPERIMENTAL RESEARCH

As a result of the research, the distribution [16] in the soil of the sliding surfaces was identified (Figure-8). The decision was very difficult. The sliding surfaces can destruct the soil. The problem is solved only by numerical methods with consideration for the weight of the soil. The line grid of the sliding surfaces has tensity for all main points including points lying on the surface of the construction site immersed into the ground. It means the known diagram of the earth pressures on the wall of

the construction site by which you can determine the force of the earth pressure.

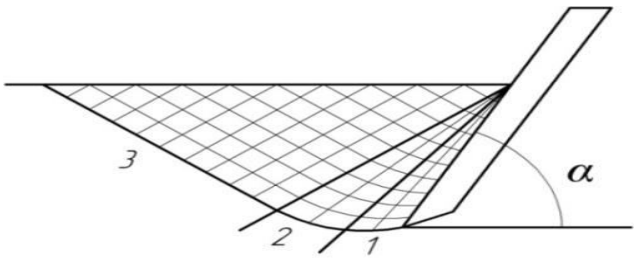

Figure-8. The grid lines of the sliding surfaces

According to the above-mentioned investigations, during the digging the chip separated from the solid mass moves up along the executive device or inside it in the form of a monolithic body. Emerging the resistance forces to the chip movement have indirect impact on the total resistance due to the increased resistance forces to the separation of the soil from the soil mass under kentledge p_o or $p(y)$. The effect of the kentledge extends on the surface in front of the moldboard blade at a distance:

$$a=h(tg\alpha+tg\psi)/(tg\alpha tg\psi),$$

where the shift angle $\psi=\pi/4-\varphi_2/2$ is assumed as a constant depending only on the internal friction angle of the soil which is contrary to the limit equilibrium theory of the loosened and cohesive environment used by the authors, in which the position and the shift surface geometries is not set in advance, but it is determined by solving the system of the differential equations of the equilibrium with certain strength conditions. At the same time, it should be noted when the kentledge occurs on the surface of the cut soil, the change of the shift angle value ψ should be expected.
The shift surfaces of the coarse cleavage shells (III) extend from the bottom part of the moldboard blade to the soil surface (Figure-9). The shift surfaces of the fine cleavage shells (I and II) come about from the same place of the moldboard blade, but extend to the surface of the previously formed coarse cleavages before reaching the surface of the soil.

The inclination angles (ψ_1 and ψ_2) to the horizon of the shift surface of the fine cleavage shells differ from the inclination angles of the coarse cleavage shells (ψ). The change of the resistance to the digging during the movement of the moldboard blade at a constant cutting depth (h) is synchronized with the phenomena of the formation process of the soil cleavages. At the time of the formation of the fine cleavage shells, the decrease of the resistance to the digging is observed and it is expressed by P_m (Figure-9). At the time of the formation of the coarse cleavage shells, the cutting force is reduced by a larger amount P_{cl} than the formation of the fine cleavage shells.

The component of the force of the resistance to the digging P_{min} is a constant value at a permanent depth of the digging. It is the result of the sum of the resistances related to the processes:

- the soil compaction by the blunt edge of the moldboard blade by the value Δh_{cm} (Figure-9) followed by its compaction into the wall;
- the overcome of the friction of the soil and the surface of the blunt edge of the moldboard blade is determined by the reaction of the elastic deformation of the compacted soil. The elastic deformation of the soil mass in front of the moldboard blade precedes to the plastic deformation of the shift or the separation of the soil cleavage element realized by the surface of the lower part of the moldboard blade which thickness is Δh_d .

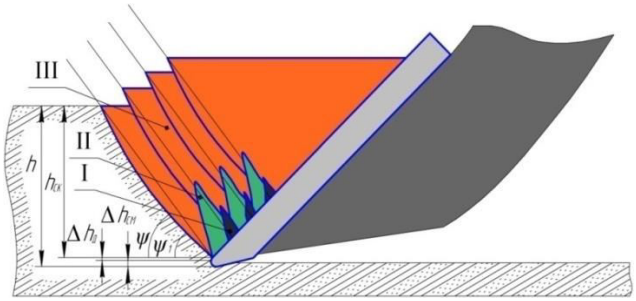

Figure-9. Scheme of the cleavage shells formation with the moldboard blade in the process of the digging

During the interaction of the blade with the soil mass, the plastic deformation of the soil with the formation of the cleavage shells occur. The shift surface in relation to the soil mass does not always reach the surface of the soil. Only coarse cleavages reach the daylight surface. At the moment of the cleavages formation there is the maximum resistance to the digging. During the movement the elements of fine and coarse cleavages move together with the previous cleavages as one body along the moldboard blade surface and the shift surface (see. Figure-9). The fine and coarse cleavages are observed at the bottom part of the moldboard blade. The plastic deformations spread from this moment. The elastic deformations of the soil mass precede to the plastic deformation of the soil mass. In the diagram the elastic deformation zone of the soil in the contact with the surface of the moldboard blade is shown by Δh_d symbol. The elastic-plastic soil compaction into the mass is done by the blunt edge of the moldboard blade and it is expressed by Δh_{cm}; Δh_{el} is the elastic deformation in the zone of the soil compaction by the blunt edge.

The maximum value of the cutting resistance corresponds to the onset of the plastic deformation of the coarse cleavages, which stems from the lower edge of the moldboard blade to the daylight surface of the soil along a plane at an angle ψ to the horizon. Thus, the developed soil mass is elastically deformed to the state in which along the plane of the development of plastic deformation the resistance force emerges. It is sufficient to overcome the

resistance to the cleavage element shift in front of the moldboard blade and along the lateral directions. It is sufficient for plastic deformation of the soil compaction into the mass by the blunt edge and the lateral sides of the moldboard blade.

In this case the maximum value of the resistance to the digging should be determined by elastic deformation of the soil mass sufficient to achieve the above-mentioned plastic deformation. According to the experimental research data, the separation of the chip from the solid mass occurs along the shift plane at the angle of ψ. For this purpose, it is necessary that in the soil mass the elastic deformation voltage reaches the sufficient value to overcome the resistance to the cleavage element formation. Before the cleavage formation in the soil mass of the elastically deformed state, the radial compressive stress σ_r occurs. The cleavage element shift occurs when the sum of the stresses acting on the shift plane intended at the angle of ψ exceeds the resistance value to the element shift.

The diagram of the forces acting on the coarse cleavage element of the soil from the side of the moldboard blade and the surface of the soil mass shift is shown in Figure 9. The daylight surface of the developed soil is horizontal for the convenience in the calculation scheme. The symbol G denotes the weight of the coarse cleavage element the value of which is determined by expression:

$$G = \frac{\gamma b h^2 \sin(\alpha + \psi)}{2\sin\alpha \sin\psi}, \quad (4)$$

where γ is the volume weight of the loosened soil kN/m^3; b is the width of the moldboard blade in m; $h_{cl} \approx h$ is the height of the cleavage element which is approximately equal to the depth of the digging because of the relatively small quantities Δh_d и Δh_{cm}; α is the soil cutting angle; ψ is the inclination angle to the horizontal surface of the coarse cleavage.

A force Q influences the cleavage element from above. It is a kentledge from the previously cleaved soil. The resultant forces of the normal N_1 and friction $F_1 = N_1 tg\varphi_1$ have an effect on the cleavage element from the side of the moldboard blade surface:

$R_1 = N_1 cos\varphi_1$,

where φ_1 is the friction angle of the moldboard blade surface.

The resultant forces of the normal N_2 and friction $F_2 = N_2 tg\varphi_2$ have an effect on the cleavage element from the side of the soil mass:

$R_2 = N_2 \cos\varphi_2$,

where φ_2 is the friction angle of the soil and soil. The traction force H_1 of the moldboard blade surface and the traction force H_2 of the soil surface effect the cleavage element from the shift surface.

$$H_1 = \frac{C_1 bh}{\sin\alpha}, \quad H_2 = \frac{C_2 bh}{\sin\psi},$$

where C_1 is the traction of the soil surface and the moldboard blade and C_2 is the traction of the soil and the soil surface of the developed soil mass.

According to the analysis of the calculation scheme with consideration for the above-mentioned forces, the resistance to the cleavage is determined by the regularity:

$$P_{rc} = \frac{(G+Q)\sin(\alpha+\varphi_1)\sin(\psi+\varphi_2)}{\sin(\alpha+\psi+\varphi_1+\varphi_2)} + [(C_1+C_2)\sin(\alpha+\varphi_2)\sin(\alpha+\varphi_1) + (C_2 \mathrm{ctg}\psi - C_1 \mathrm{ctg}\alpha)\sin^2(\alpha+\varphi_1)\cos(\psi + \varphi_2)]\frac{bh}{\sin(\alpha+\psi+\varphi_1+\varphi_2)} + C_1 bh \mathrm{ctg}\alpha. \quad (5)$$

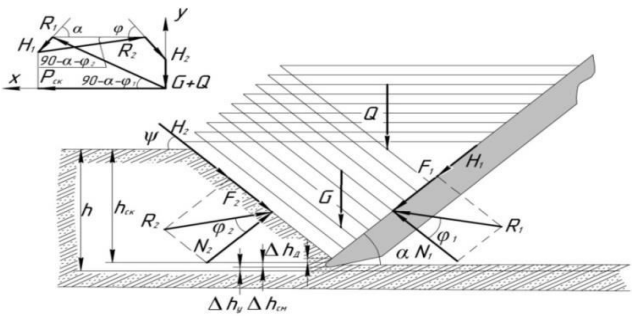

Figure-10. The forces acting on a soil cleavage element

If we do not take into account the soil traction and the moldboard blade surface and the soil mass surface ($C_1 = C_2 = 0$) and the value of the kentledge from the previous cut soil ($Q = 0$), then the formula becomes a formula of G. N. Karasev [19].

The calculation scheme shown in Figure 9 is used to determine the resistance force to the elastic deformation of the soil mass until the formation of the plastic deformation of the cleavage element separation.

Here we use a method similar to the method of the stresses distribution determination from the action of the concentrated force at any point of the elastic half-space. In our case, the effect on the elastic half-space can be represented in the form of specific linear load equally distributed across the width of the moldboard blade (R_{ef}, H/m) acting from the lower edge of the moldboard blade on the soil mass perpendicular to the plane oriented to the horizon at an angle ($\alpha + \varphi_1$) (Figure-10). The orientation of this force is determined by the nature of the interaction with the soil surface and the moldboard blade, because at the point of contact with the soil, a normal surface emerges to the surface of the moldboard blade, and frictional force acts in the direction opposite to the movement of the soil. The point A inside the soil mass is defined by polar coordinates r and β. The line of the surface will be drawn through the point A perpendicular to

r and define the value of the normal stress σ_r, acting on the surface.

The displacement of the point A in the direction of radius r will be considered. The farther away from the point of application of the linearly distributed force R_{ef} the point A will be located, the smaller its displacement will be. At the same value r, the displacement of the points corresponding to the different angles β will be different. The maximal displacement will be in the direction of the line of effect force R_{ef} (at $\beta = 0$). The displacement of the points will decrease with an increase of the angle β, and the displacement of the points will be equal to zero in the limited plane (at $\beta = 90°$). From these considerations it is assumed that the displacement of the point A in the direction of radius r is equal to

$$S_A = \frac{(\nu\cos\beta)}{r}, \tag{6}$$

where ν is the coefficient of proportionality.

It is supposed that point A has displaced to point B at a distance dr. The deformation e_r in the relation to the segment dr will be defined. The displacement of the point B like the previous one is defined by the expression:

$$S_B = \frac{(\nu\cos\beta)}{(r + dr)}. \tag{7}$$

Then the relative deformation of the segment is equal to dr

$$e_r = \frac{(S_A - S_B)}{dr} = \left[\frac{\nu}{r} - \frac{\nu}{(r + dr)}\right]\frac{\cos\beta}{dr} = \frac{\nu\cos\beta}{(r^2 + rdr)}. \tag{8}$$

Neglecting the value rdr in the denominator of this expression, which is insignificant in comparison with r^2,we obtain

$$e_r = \frac{(\nu\cos\beta)}{r^2}. \tag{9}$$

And since between the stress and strain the direct proportionality is taken, the value of the radial stress, which causes the relative compression of the considered element, will be equal to

$$\sigma_r = \frac{\xi\nu\cos\beta}{r^2}, \tag{10}$$

where ξ is the proportionality factor.

The product of $\xi\nu$ coefficients is determined by the equilibrium conditions. To compile the equilibrium equations and to determine the voltage σ_r, the section of the half-cylinder which axis coincides with the cutting edge of the moldboard blade will be considered. The sectional plane of semi-cylinder is perpendicular to the force vector R_{ef} crossing the cylinder axis. Across the surface of the semi-cylinder compressive stresses σ_r will be applied. The value of the compressive stresses is expressed by the above-mentioned formula. The value of the strain is considered equal to the elementary area with the width dl corresponding to the central angle $d\beta$ and radius r. From the equilibrium condition it follows that the sum of the projections of all forces in the direction of the vector R_{ef}, which is perpendicular to the plane bounding linearly deformable soil mass, must be equal to zero, i.e.

$$R_{ef} - 2\int_0^{\frac{\pi}{2}}\int_0^{l}\sigma_r\cos\beta r d\beta dl = 0 .$$

Substituting the value σ_r, we get

$$2\int_0^{\frac{\pi}{2}}\cos^2\beta d\beta = [\cos\beta\sin\beta + \beta] .$$

Considering

$$R_{ef} = \frac{2\nu\xi l}{r}\int_0^{\frac{\pi}{2}}\cos^2\beta d\beta ,$$

we obtain

$$R_{ef} = \frac{\nu\xi\pi l}{2r}. \tag{11}$$

From this expression we define the product of the coefficients:

$$\nu\xi = \frac{2R_{ef}r}{\pi l}. \tag{12}$$

Substituting the value $\nu\xi$ in the formula for the radial stresses, we finally obtain

$$\sigma_r = \frac{2R_{ef}\cos\beta}{\pi r l}. \tag{13}$$

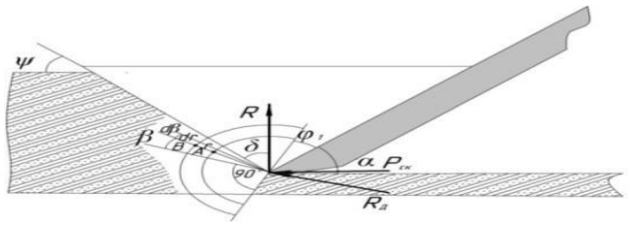

a)

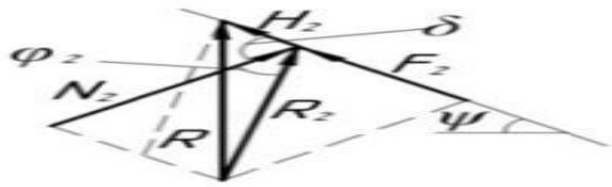

b)

Figure-11. The scheme of distribution of forces in the elastic half-space

Now the diagram of forces applied to the coarse elements of cleavage will be considered. The shift surface of the cleavage reaches the daylight surface of the soil mass. At the time preceding the process of cleavage element separation from the soil, mass plastic deformation emerges along the shift surface oriented at an angle to the surface ψ (Figure-11a). The rest of the soil mass is deformed elastically as indicated by many researchers in their works [19, 20].

To implement the plastic deformation of the separation of the coarse element of the cleavage at the angle ψ, it is necessary to overcome the resistance of the forces of friction and cohesion in the shift plane as well as the weight of the cleavage element G and kentledge Q from the previous cut-off soil. The diagram in Figure 10b shows the resulting vector R corresponding to these resistances. The value of this force vector is determined according to the calculation model by the expression:

$$R = \sqrt{N_2^2 + (F_2 + H_2)^2}\,, \tag{14}$$

where

$$N_2 = \frac{(Q+G)\sin(\alpha+\varphi_1)\cos\varphi_2}{\sin(\alpha+\psi+\varphi_1+\varphi_2)}\,;$$

$$F_2 = \frac{(Q+G)\sin(\alpha+\varphi_1)\sin\varphi_2}{\sin(\alpha+\psi+\varphi_1+\varphi_2)}\,;$$

$$H_2 = \frac{C_2 bh}{\sin\psi}.$$

The direction of the vector operation with respect to the cleavage plane is characterized by the angle δ between the vector R and the cleavage plane of the shift element defined by the expression:

$$\delta = \arcsin\frac{N_2}{R}.$$

The plastic deformation is preceded by the elastic deformation in the process of which the potential energy is accumulated. The part of the energy is released in the course of the implementation of the plastic deformation. This potential energy of the elastic deformation of the soil mass is created by the radial compressive stresses in the angular range between the shift surface and angle characterized by ψ, and the plane bounding the linear deformable soil mass, i.e. the plane defined by the angle $(\alpha + \varphi_1)$ in Figure-11a. The angle β varies in this range from $\beta=\alpha+\varphi_1+\psi-\pi/2$ to $\beta=\pi/2$. The amount of projection of the radial compressive stresses $\sigma_r(\beta)$ in the specified angular range β in the direction of the operation of the vector R provides the fulfillment of its value sufficient for the plastic deformation of the cleavage element separation of the soil at an angle ψ. In this case, the following equation can be written:

$$R = \int_0^l \int_\rho^{\pi/2} \sigma_r \cos[\delta - (\beta - \rho)]\,r\,d\beta\,dl = \int_0^l \int_\rho^{\pi/2} \sigma_r \cos[\delta + (\beta - \rho)]\,r\,d\beta\,dl\,, \tag{15}$$

where $\rho=\alpha+\varphi_1+\psi-\pi/2$.

Substituting the value in this expression $\sigma_r=(2R_{ef}\cos\beta)/(\pi r l)$, we obtain the equation:

$$R = \frac{2R_{ef}}{\pi}\int_\rho^{\pi/2} \cos\beta\cos(\delta+\rho+\beta)\,d\beta\ .$$

After solving the integral and the corresponding transformations, we obtain

$$= R_{ef}\frac{\sin(\delta+\alpha+\varphi_1+\varphi_2)[\pi-\alpha-\varphi_1-\psi+0{,}5\sin 2(\alpha+\varphi_1+\psi)]}{\pi} - \frac{\cos(\delta+\alpha+\varphi_1+\psi)\sin^2(\alpha+\varphi_1+\psi)}{\pi}$$

We introduce

$$A = \frac{\sin(\delta+\alpha+\varphi_1+\psi)[\pi-\alpha-\varphi_1-\psi+0{,}5\sin 2(\alpha+\varphi_1+\psi)]}{\pi} - \frac{\cos(\delta+\alpha+\varphi_1+\psi)\sin^2(\alpha+\varphi_1+\psi)}{\pi}.$$

Then we have

$$R_{ef} = \frac{R}{A}\,. \tag{16}$$

As a result, we have the formula for determining the maximum value of cutting resistance and the resistance to the elastic deformation of the soil mass:

$$R_{ef} = \frac{R\sin(\alpha+\varphi_1)}{A}\,. \tag{17}$$

For the case of the soil cutting which does not stick to the moldboard blade (H_1=0)

$$P_{rc} = R_{ef}\sqrt{\frac{(Q+G)^2\sin^2(\alpha+\varphi_1)\cos^2\varphi_2}{\sin^2(\alpha+\psi+\varphi_1+\varphi_2)} + \left(\frac{(Q+G)\sin(\alpha+\varphi_1)\sin\varphi_2}{\sin^2(\alpha+\psi+\varphi_1+\varphi_2)} + \frac{C_2 bh}{\sin\psi}\right)^2}, \tag{18}$$

For the case of cutting of the loosen soil when $C1=C2=0$

$$P_{rc} = \frac{(Q+G)\sin^2(\alpha+\varphi_1)}{A\sin(\alpha+\psi+\varphi_1+\varphi_2)}\,. \tag{19}$$

The total resistance to the cutting with the resistance to the cleavage and the soil compression by the cutting edge of the moldboard blade without the resistance to the formation of the side cleavage shells for flat blades without teeth is determined by the dependence:

$$= \frac{\sin(\alpha+\varphi_1)}{A}\sqrt{\frac{(Q+G)^2\sin^2(\alpha+\varphi_1)\cos^2\varphi_2}{\sin^2(\alpha+\psi+\varphi_1+\varphi_2)} + \left(\frac{(Q+G)\sin(\alpha+\varphi_1)\sin\varphi_2}{\sin^2(\alpha+\psi+\varphi_1+\varphi_2)} + \frac{C_2bh}{\sin\psi}\right)^2} ++ \frac{Ksl\sin\alpha}{0{,}5\pi\,\mathrm{tg}\,(\alpha-\varphi_1)+\cos(\alpha-\varphi_1)}. \quad (20)$$

Physicochemical properties of soils depend on their state and conditions of interaction with manipulators. Dependences of soil properties were discussed in details in [21-24], herewith, it is recommended to determine their values using multifactor models.

The developed mathematical model makes it possible to determine variation of forces of normal and tangential pressures during "manipulator-soil" interaction using the predefined multifactor functions with accounting for manipulator geometrical parameters, physicomechanical properties of soil, speed of load application, soil weight constrained by planes of sliding and load distributed over bulk surface.

RESULTS

Based on the optimization of existing prediction procedures of soil resistance against cutting, the mathematical model was derived (2.14) accounting for cutting determinant factors. Peculiar feature of this model is accounting for shape of sliding surface upon prediction of sliding body volume using CAD software.

The applied CAD software was adapted to solution to soil cutting problem. With this aim, the initial model of processed soil was developed, the applied cutting manipulator was simulated individually, the initial data included the physicochemical properties of soil. Then, the step was determined allowing to perform predictions with minimum time losses and providing satisfactory accuracy of resulted data. Each step was completed with generation of files with predicted results, these files were processed and presented in user friendly form by the same software. Computer simulation made it possible to visualize movements of units under the action of applied loads, stress isolines, shear stresses, deformation intensity, elements reaching plasticity state, as well as some other special properties (see Figure-12).

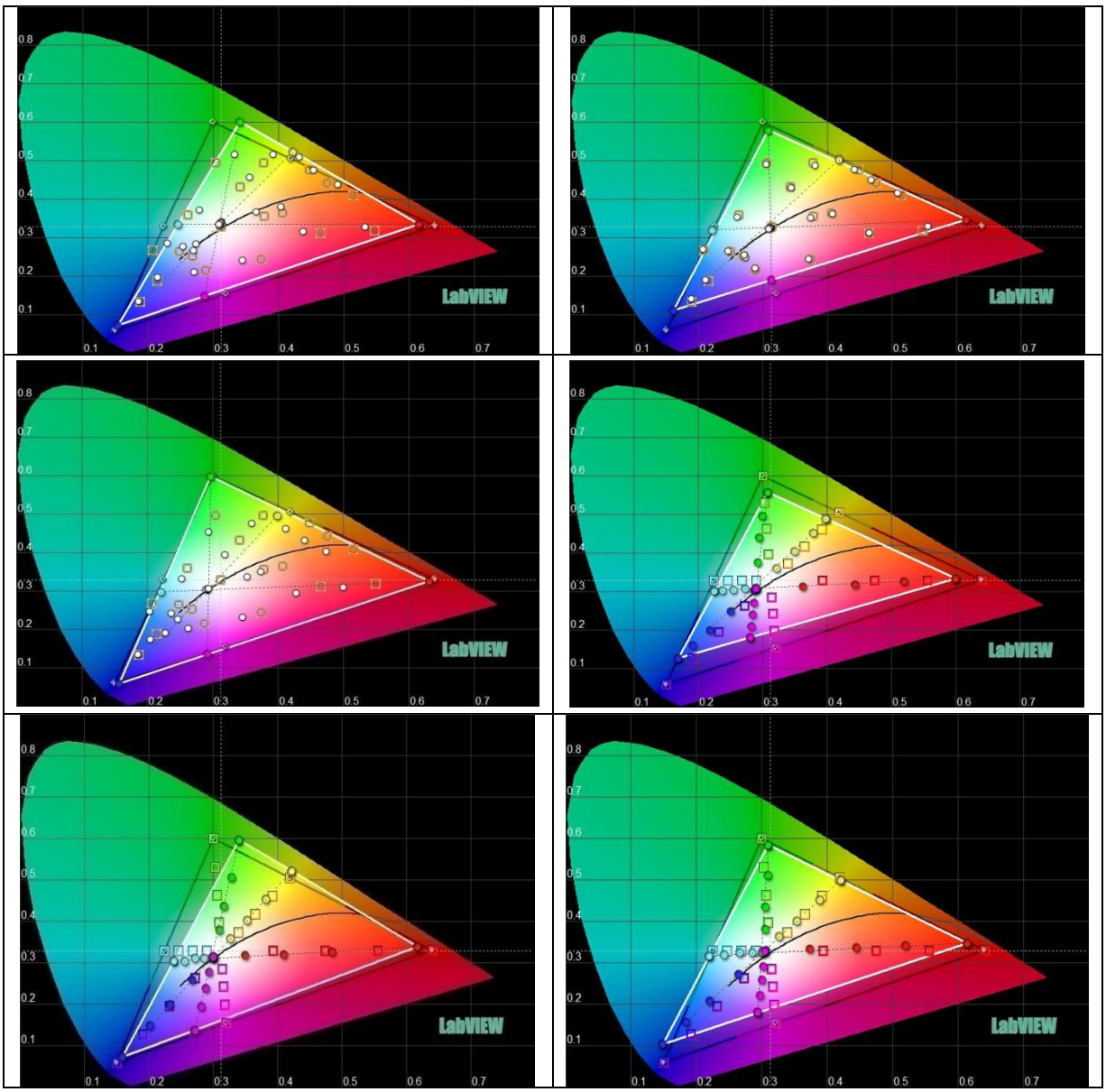

Figure-12. Isolines of temperature–shift stresses and deformation upon soil cutting with accounting for sliding surface.

The considered process can be controlled by a user at each step or in preset number of steps by displaying or printing of images of initial and deformed models, schemes of fixation or application of loads, finite element grid, isotherms and profiles, highlighted areas of plasticity and imperfections.

Additional software was developed for analysis of the obtained results accounting for peculiar features of soils, the criterion of continuity breaking, in particular. In addition, it is possible to convert the predictions into AutoCAD, which enables to use its options for further data processing and printing.

During simulation the contact conditions are continuously updated reflecting internal strength properties of processed soil, thus allowing to simulate sliding between manipulator and tested material (see Figure 13). 3D geometrical model of manipulator was plotted in CAD program, Inventor, and imported into CAE program.

Application of this software made it possible to determine development of area of ultimate plastic state of soil bulk by iteration of external load, and its exit onto soil surface predetermined direction of its migration upon further loading, i.e. from sliding surface.

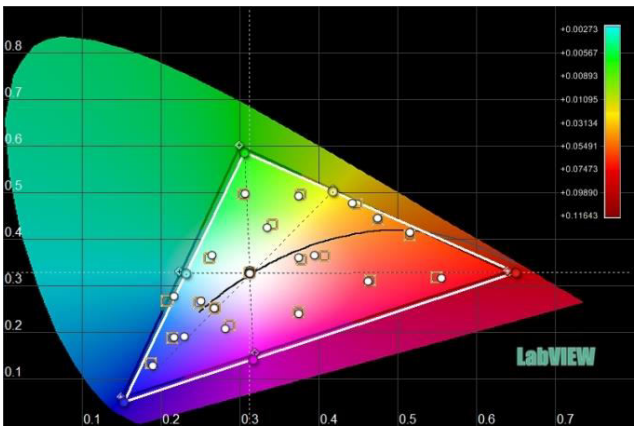

Figure-13. Ultimate plastic state of soil bulk upon iteration of external load.

The results of the analysis of the obtained formula are given in comparison with the results of calculations by the empirical formula of Professor A. N. Zelenin. The calculations were made for a variety of soils which characteristics are shown in Table-3 for the case of the kentledge lack Q=0.

Table-3. The characteristics of soils.

Parameters	Sand	Sandy loam	Clay loam	Clay
φ_1^o	27	27	29	33
φ_2^o	35	35	39	42
C_2, daN/m^2	0	1,000	3,000	6,000
C, specific	1	6	12	16

The dependence of the cleavage angle ψ on the cutting angle is shown in Figure 11b. It means that the soil cleavage angle for different soils decreases when the cutting angle α increases. The meaning of the cleavage angle presented in this graph corresponds to the minimum resistance of the soil chip separation from the soil mass, i.e, the minimum energy consumption of the soil cutting process.

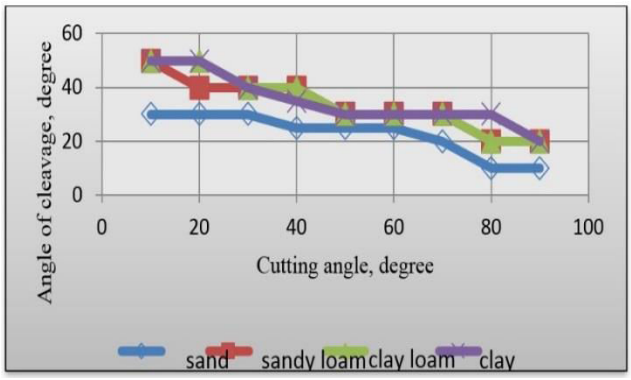

Figure-14. The dependence of the angle of cleavage on the cutting angle for different soils

The dependence of the resistance to the cutting of sand, sandy loam, clay loam, and clay on the angle of the cutting by blade with the width of 1 m to the depth of 0,01 m is shown in Figures 15, 16. The graph also shows the value of the cutting resistance calculated by the formula of Professor A. N. Zelenin, which corresponds to the results of experimental studies. The results of the theoretical calculations (Tables 4, 5) correspond to the soil cleavage angle according to the schedule defined by $\psi = f(\alpha)$ (Figure-15). The satisfactory convergence of the results of comparison of the calculated and experimental cutting resistance of various soils in the range of the cutting angle from 30° to 70° corresponding to the practical range of applied angles of cutting for the blades of the executive devices of the earthmoving machinery should be noted.

The graphs of the change in resistance to cutting soil depending on the depth of the cut with a blade at the cutting angle of 30^0 and with the width of 100 cm are shown in Figure-16. The calculated data with the use of the theoretical formula are compared with experimental data obtained by calculation according to the empirical formula of Professor A. N. Zelenin. Analyzing these materials, it is necessary to state the good and satisfactory convergence of matched data for the relatively soft soils (sand and sandy loam) with the number of strokes of the dynamic densitometer F having from 1 to 6 strokes, and the significant difference for the solid soil (loam and clay) with the number of strokes F from 12 and above.

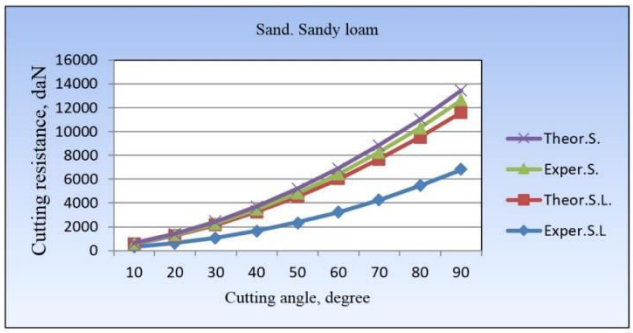

Figure-15. Cutting resistance depending on angle of cut

Table-4. Results of theoretical and experimental research.

Sand, daN C=1, H=0,01 m									
theoretical	41	104	181	267	360	461	569	680	798
experimental	32	61	113	190	295	431	601	806	1,050
Sandy loam, daN C=6, H=0,01 m									
theoretical	246	628	1,086	1,602	2,165	2,770	3,411	4,084	4,788
experimental	323	633	1,074	1,651	2,371	3,240	4,262	5,446	6,795

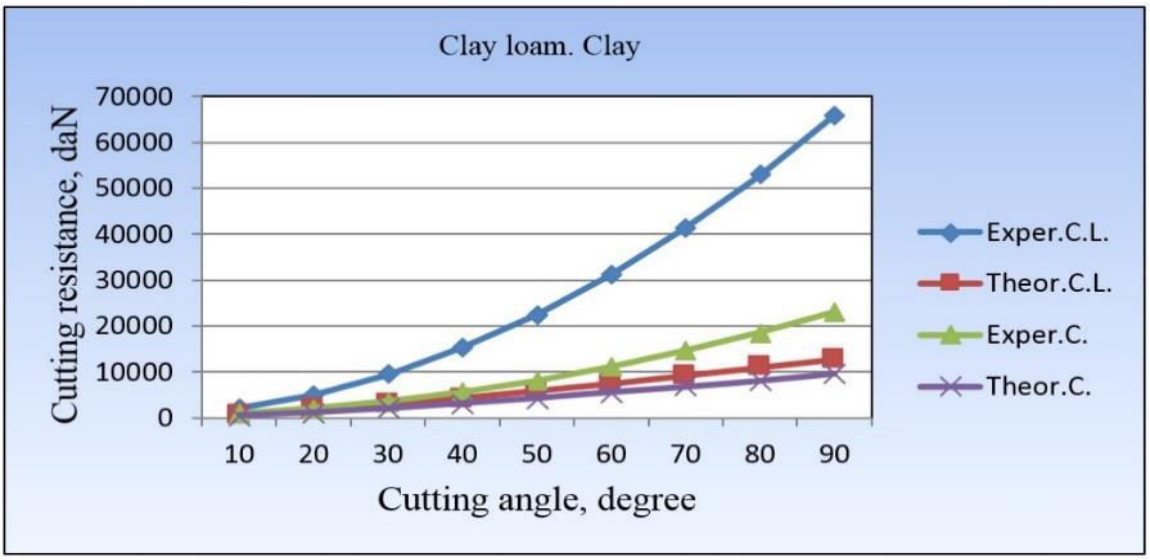

Figure-16. Cutting resistance depending on angle of cut

Table-5. Results of theoretical and experimental research.

Clay loam, daN C=12, H=0,01 m									
theoretical	493	1,257	2,173	3,204	4,331	5,540	6,822	8,169	9,577
experimental	919	2,009	3,569	5,605	8,125	11,135	14,643	18,654	23,176
Clay, daN C=16, H=0,01 m									
theoretical	657	1,676	2,898	4,273	5,775	7,387	9,096	10,983	12,770
experimental	2,093	5,034	9,433	15,246	22,484	31,158	41,279	52,858	65,906

As mentioned above, the reliability of theoretical studies is confirmed by substantiated use of fundamental dependences, assumptions and limitations, correct formulation of mathematical simulation, application of modern mathematical methods and hardware.

Qualitative and quantitative coincidence of theoretical results with experimental data obtained in wide range of technological modes of the considered process confirms the reliability of the obtained results even more. Aiming at more complete prove of reliability of the obtained results, laboratory experiments have been carried out.

The experiments have been aimed at verification of theoretical studies of chip formation by determination of functional dependences of sliding surface shape as applied to the most common soil types as well as at evaluation of effect of factors of cutting on the pattern of chip formation.

CONCLUSIONS

The experimental studies of active interaction with shift on the manipulator model confirm validity of the proposed physics of soil cutting. Accounting for sliding surfaces in predictions of soil resistance against cutting makes it possible to improve accuracy of predictions and explain the cutting essence as a function of soil type.

The shape of sliding surface and the chip sizes depend to various extents on factors characterizing the

process of cutting. Thus, when cutting angle decreases from 60° to 30°, the transversal surface area of chips increases by up to 20%, and upon increase in drawing prism weight, the transversal surface area of chips increases by 3-17% depending on soil type. Increase in cutting speed from 0.5 m/s to 5 m/s in the range of operation speeds of earth-moving machines does not exert significant effect on chip formation and sizes of sliding bodies (up to 8%).

The shapes of sliding surface obtained during simulation and full-scale experiments as well as the results based on finite element model of soil are identical, which facilitates their functional description depending on soil type.

The mathematical model of active interaction of manipulators with medium agrees with the experimental results. It allows to determine occurring resistances of bucket and earthmoving manipulators, side knives upon active interaction with shift with the accuracy up to 10%.

REFERENCES

[1] Polosin M. D. 2002. Mashinyst dorozhnyh I stroitelnyh. Moscow: Izdatelskii centr “Akademia. p. 288.

[2] Berestov E. I. 1998. Nauchnye osnovy modelirovanya sistemy “grunt-rabochie organy zemleroinyh mashyn” v rezhime posloinoi razrabotky: Avtoref. dis. d.t.n. Mogilev.

[3] Gruzin A. V., Gruzin V. V., Abramenkov E. A. 2009. Gruntjvye sredy v uslovyah staticheskogo i dinamicheskogo nagruzhenya. Omsk: Izd-vo OmGTU. p. 140.

[4] Goryachev M. G. 2003. Raschet proizvoditelnosty mashin dlya stroitelstva, remont i soderzhanya gorodskih putey soobshenia. Moscow: MKLP. p. 36.

[5] Lutov V. N. Sartakov A. V. 2011. Kompleksnaya mehanyzacya tehnologicheskih processov v stroitelno-dorozhnom proizvodstve: uchebnoe posobie. Barnaul: Izd-vo AltGTU. p. 166.

[6] Abramenkov D. E. *et al.*, Kima B. G. (Ed.). 2004. Stroitelnye mashiny: ucheb.posobie. Vladimir: Red.-izdat. Kompleks VlGU. p. 190.

[7] Zelenin A. N., Balovnev B. Y., Kerov I. P. 1975. Mashiny dlya zemlyanyh rabot. M.: Mashinostroenie. p. 423.

[8] Permykov V. B. 2008. Kompleksnaya mehanizacia stroitelstva. Moscow: Vysh. Shk. p. 382.

[9] Karlsson L. 1999. Welding in the World. 43: 20.

[10] Josefsson B., Nilsson J. O., Wilson A. 1991. Proc. Duplex Stainless Steels'91. Les Editions de Physique. Les Ulis Cedex. France. p. 67.

[11] Stanevski V. P., Khmara L. A., Kolesnikov N. P. 1992. Modernizacya I povyshenie proizvoditelnosty stroitelnyh mashyn. Kiev: Budivelnik. p. 152.

[12] Balovnev V. Y. 2008. Avtomobili i traktory. Kratky spravochnik. Moskva-Omsk: Izd-vo SibADI. p. 383.

[13] Balovnev V. Y., Glagolev S. N., Danilov R. G., Kustarev G. N., Shestopalov K. K., Gerasimov M. D. 2011. Mashiny dlya zemlyanih rabot: Konstrukcya, raschet, potrebitelckie svoistva. Belgorod: Izd-vo BGTU. p. 401.

[14] Surashev N., Dudkin M. V., Yelemes D., Kalieva A. 2013. The Planetary Vibroexciter with Elliptic Inner Race. Trans Publications, Switzerland, Advanced Materials ResearchVols. 694-697: 229-232.

[15] 15Pichugin S. Yu., Dudkin M. V., Fadeev S. N. 2013. Contact Force Calculation of the Machine Operational Point. Life Science Journal. 10(10s): 246-250.

[16] Turusbekov K., Tusupbekov M., Khon N., Gabdysalyk R., Turusbekov S., Zhailaubaev D. 2015. The Improvement of the digging process with the sliding surface consideration. Biosciences Biotechnology Research Asia, December. 12(3): 2995-3008.

[17] Pichugin S. Yu., Dudkin M. V., Fadeev S. N. 2013. The Analysis of Road Machine Working Elements Parameters. World Applied Sciences Journal. 23(2): 151-158.

[18] Vavilov A. V., Pichugin S. Yu., Dudkin M. V., Fadeev S.N. 2013. Calculation of the Interaction of Working Body of Road Machine with the Surface. Life Science Journal. 10(12s): 832-837.

[19] Karasev G. N. 1970. Vybor osnovnyh parametrov pricepnogo screpera. Dissertacya na soiskanie uchenoi stepeny kand. tehn. nauk. Moscow: MADI.

[20] Shestopalov K. K. 2005. Podiemno-transportnye, stroitelnye i dorozhnye mashyny I oborudovanye. Moscow: Izdatelsky centr “Akademya. p. 320.

[21] Sokolov G. K. 2008. Tehnologia stroytelnogo proyzvodstva. Moscow: Akademia. p. 539.

[22] Doudkin M., Kim A., Kim V., Mlynczak M., Kustarev G. 2018. Computer Modeling Application for Analysis of Stress-strain State of Vibroscreen Feed Elements by Finite Elements Method. Mathematical Modeling of Technological Processes International Conference, CITech 2018, Ust-Kamenogorsk, Kazakhstan, September 25-28, Proceedings. pp. 82-96. https://doi.org/10.1007/978-3-030-12203-4_9.

[23] Bostanov B. O., Temirbekov E. S., Dudkin M. V., Kim A. I. 2018. Mechanics-Mathematical Model of Conjugation of a Part of a Trajectory with Conditions of Continuity, Touch and Smoothness. Mathematical Modeling of Technological Processes International Conference, CITech Ust-Kamenogorsk, Kazakhstan. September 25-28, 2018. Proceedings. pp. 71-81. https://doi.org/10.1007/978-3-030-12203-4_8.

[24] Doudkin M., Kim A., Kim V. 2019. Application of FEM Method for Modeling and Strength Analysis of FEED Elements of Vibroscreen. Proceedings of the 14th International Scientific Conference on Computer Aided Engineering, June 2018. Series: Lecture Notes in Mechanical Engineering. Wrocaw, Poland. p. 892.